Pacific–East Asian Teleconnection. Part II: How the Philippine Sea Anomalous Anticyclone is Established during El Niño Development*

BIN WANG AND QIN ZHANG

Department of Meteorology, School of Ocean and Earth Science and Technology, University of Hawaii at Manoa, Honolulu, Hawaii

(Manuscript received 12 November 2001, in final form 4 March 2002)

ABSTRACT

The *anomalous* Philippine Sea anticyclone (PSAC) conveys impacts of El Niño to east Asian climate during the mature and decay of an El Niño (from the winter to ensuing summer). It is shown that the anomalous PSAC forms in fall about one season prior to the peak El Niño; its strength increases with the El Niño intensity and its sign reverses during a La Niña. The PSAC formation concurs with abnormal deepening of the east Asian trough and with increasing number of northward recurvature of tropical storms in the western Pacific. The PSAC establishment is abrupt, coupling with a swing from a wet to dry phase of an intraseasonal oscillation (ISO) and often concurrent with early retreat of the east Asian summer monsoon. The ISO becomes inactive after PSAC establishment.

The development of the PSAC is attributed to combined effects of the remote El Niño forcing, tropical–extratropical interaction, and monsoon–ocean interaction. The developing El Niño induces off-equatorial ascending Rossby wave responses and land surface cooling in northeast Asia; both deepen the east Asian trough in fall and induces vigorous tropical–extratropical exchange of air mass and heat, which enhances the cold air outbreak and initiation of the PSAC. Through exciting descending Rossby waves, the El Niño–induced Indonesian subsidence generates low-level anticyclonic vorticity over south Asia, which is advected by mean monsoon westerly, instigating the anomalous PSAC. The ISO interacting with the underlying ocean plays a critical role in the abrupt establishment of PSAC. The wind–evaporation/entrainment feedback tends to amplify (suppress) ISO before (after) winter northeasterly monsoon commences, suggesting the roles of *atmosphere–ocean interaction* and the seasonal march of background winds in changing the Philippine Sea ISO intensity and maintaining PSAC.

1. Introduction

The Chinese mei-yu and Japanese baiu in June and July are associated with a major rain producing system—the east Asian subtropical front. For more than a decade, scientists have recognized that mei-yu rainfall increases significantly in the summer after an El Niño (e.g., Huang and Wu 1989; Lau and Yang 1996; Zhang et al. 1996; Kawamura 1998; Tao and Zhang 1998). The devastating Yangtze River flood in the summer of 1998 that followed on the heels of the 1997 El Niño is such an example. El Niño episodes, however, mature usually in boreal winter, and by the next summer the warming in the equatorial central-eastern Pacific normally disappears. How then does El Niño have its ''delayed'' influence on the east Asian summer monsoon? Wang et al. (2000) have pointed out that the circulation system that conveys the impact of El Niño to east Asia is an anomalous low-level anticyclone located over the Philippine Sea [the Philippine Sea anticyclone (PSAC)]. The PSAC persists from the mature El Niño to the ensuing summer, strengthening the western Pacific subtropical ridge in early summer, which then causes the abundant precipitation in the lower reach of the Yangtze River valley. Given the chaotic nature of atmospheric motion and the decaying remote forcing by El Niño, what mechanisms sustain the PSAC for three seasons? Wang et al. (2000) have put forth a theory that attributes the persistence of the PSAC to positive thermodynamic feedback between atmospheric descending Rossby waves and the underlying cold SST anomaly to the east of the PSAC center. This positive feedback operates in the presence of background northeasterly monsoon or trade winds. To the east of the anomalous PSAC, the increased total wind speed cools the ocean surface where it induces excessive evaporation and entrainment. The cool-

* School of Ocean and Earth Science and Technology Publication Number 6024 and the International Pacific Research Center Publication Number 173.

Corresponding author address: Dr. Bin Wang, Department of Meteorology, and the International Pacific Research Center, University of Hawaii at Manoa, 2525 Correa Road, Honolulu, HI 96822.
E-mail: bwang@soest.hawaii.edu

© 2002 American Meteorological Society

ing, in turn, suppresses convection and reduces latent heating in the atmosphere, which excites descending atmospheric Rossby waves that reinforce the PSAC in their decaying journey to the west.

The work of Wang et al. (2000) was focused on the teleconnection in mature and decay phases of El Niño. Issues remain as to (i) when and how the PSAC is established during the El Niño development, and (ii) what processes are responsible for the formation of the PSAC. The present work is a continuation of Wang et al. (2000), aiming at addressing these questions. For this purpose our analyses focus on the El Niño developing phase in the summer and fall of the El Niño years.

In section 2, we describe the datasets and the analysis method used in this study. A typical scenario of the PSAC formation and evolution during an El Niño event are documented in section 3. In sections 4, 5, and 6, we examine the possible factors that contribute to the PSAC formation, including the effects of remote El Niño forcing, extratropical–tropical interaction, and local air–sea interaction associated with intraseasonal oscillation (ISO). We found that during the fall of the El Niño development years, the remote El Niño forcing intensifies the east Asian trough and reinforces tropical storm activity over the western North Pacific (WNP). The enhanced tropical–extratropical interaction over east Asia and WNP favors the initiation and development of the PSAC. Meanwhile, the ISO and local air–sea interaction play a critical role in suddenly establishing and in maintaining the PSAC. The last section presents a summary.

2. Data and method

The main datasets used are daily, pentad, and monthly mean National Centers for Environmental Prediction–National Center for Atmospheric Research (NCEP–NCAR) global atmospheric reanalysis data from January 1957 to December 1999 (Kalnay et al. 1996). The variables include sea level pressure, precipitation, surface temperature and fluxes, 500-hPa geopotential height, and winds at 200 hPa, 850 hPa, and the surface. The anomalous fields are obtained by removing the long-term mean and annual cycle. The interannual variation associated with ENSO is represented by 7-pentad running mean anomalies. The departure of the pentad mean anomalies from the corresponding 7-pentad running mean was used to denote ISO components and to describe the rapid establishment of the PSAC.

The Joint Typhoon Warning Center (JTWC) western North Pacific tropical cyclone best-track data from 1950 to 1999 were used to examine the influence of the El Niño and La Niña during the anomalous PSAC formation period.

Our strategy is to focus on common features of the six strongest El Niño episodes (1957/58, 1965, 1972, 1982/83, 1991/92, and 1997/98) in contrast to six major La Niña episodes (1970/71, 1973, 1975, 1988, 1998, and 1999) by using the composite technique. One-sample and two-sample Student's *t* tests are used to establish statistical significance of the composites.

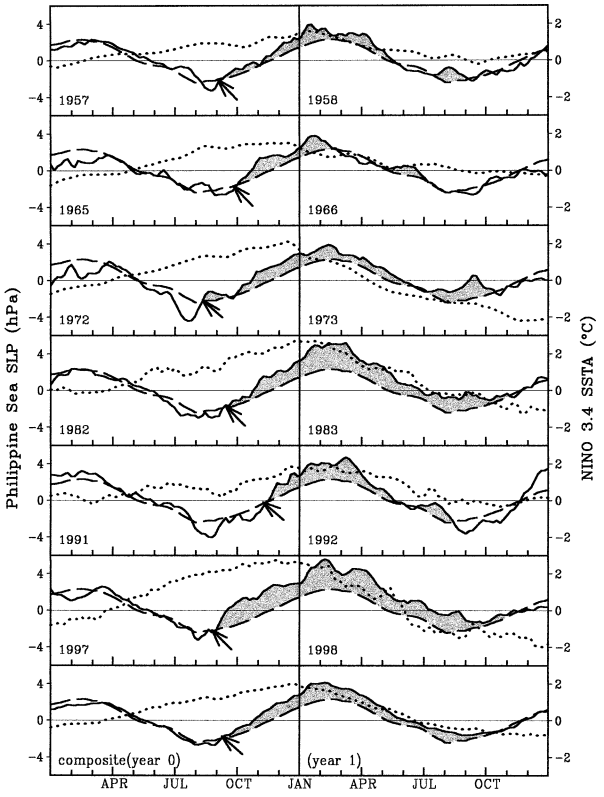

FIG. 1. The 7-pentad running mean (solid) and the climatological annual cycle (excluding the annual mean; long dashed) sea level pressure averaged over the Philippine Sea (10°–20°N, 120°–150°E) for six major El Niño episodes and their composite with reference to the calendar month. The dotted curves are the corresponding 3-month running mean Niño-3.4 SST anomalies. The arrows indicate the time that the anomalous PSAC occurs. The shading highlights the period during which the PSAC persists.

The sea surface temperature (SST) in the NCEP–NCAR reanalysis uses Reynolds reconstructed monthly mean SST (Reynolds and Smith 1994) after 1982 and the Global Sea Ice and Sea Surface Temperature dataset (GISST) before 1982. In order to examine the sudden establishment process of the anomalous PSAC and associated air–sea interaction process, we used only the data after 1982 during which the daily data are more reliable due to usage of high-resolution satellite observations. To enhance the reliability, pentad anomalies were constructed from the daily precipitation, skin temperature over the sea and land surfaces, and the surface latent heat and downward solar radiation fluxes.

3. Formation of the anomalous Philippine Sea anticyclone

The climate over the Philippine Sea is of typical monsoon character. As shown by the long dashed lines in Fig. 1, the sea level pressure (SLP) averaged over the

Philippine Sea (10°–20°N, 120°–150°E) is dominated by an annual cycle. The SLP drops below the annual mean in early May and remains below until mid-November. Likewise, the winds and precipitation also exhibit a dominant annual cycle (Murakami and Matsumoto 1994; Wang 1994; Wu and Wang 2000). The seasonal transition from summer to winter occurs in November, which is about two months after the corresponding transition in subtropical east Asia (mid-September).

When does the PSAC get established during the El Niño developing year? Figure 1 indicates that the SLP over the Philippine Sea rises from below to above normal in the fall of an El Niño–developing year with an *average date* in early October (the arrows in Fig. 1), following the withdrawal of the east Asian summer monsoon. The formation of the PSAC implies rapid weakening of the WNP monsoon trough, or advance of seasonal transition in the WNP, on average, by about one month (see the composite diagram in Fig. 1). In the mature phase of El Niño, the SLP anomaly reaches 2 hPa, which is comparable to the amplitude of the local annual variation. The intensity of the PSAC is more pronounced in the events after the late 1970s, possibly associated with the amplification of the El Niño–Southern Oscillation (ENSO) cycle (Gu and Philander 1997; Wang 1995).

Is the establishment of the PSAC anomaly a local phenomenon? How do the pressure anomalies evolve? Figure 2 displays the monthly mean SLP and SST anomalies averaged along a latitudinal band between 10° and 20°N. Around September (0), where 0 means the year during which an El Niño develops, significant positive SLP anomalies (0.5 hPa) commence nearly simultaneously across south Asia from India to about 130°E. In October, the SLP anomalies reach 1 hPa near the Philippines (120°E). Thus, the rising pressure is not a local event but associated with large-scale seasonal changes of the Asian monsoon system, especially the South China Sea monsoon. The center of the PSAC shows an eastward shift from 120° in October (0) to 152°E in February (1) with a speed about 8° longitude per month. This eastward displacement is accompanied by significant development of negative SST anomalies to the east and positive SST anomalies to the west of the PSAC. Both the SLP and negative SST anomalies (SSTA) extend eastward in a coherent manner, suggesting a coupling between the PSAC and SSTA as suggested by Wang et al. (2000). The numerical experiments performed by Lau et al. (2002, hereafter LNW) with a coupled atmospheric general circulation model and a mixed layer ocean model show a similar coherent eastward propagation of SST and SLP anomalies, which is a manifest of the air–sea coupling.

Figure 3 shows that the abruptness of the PSAC formation is associated with a shift from a low pressure to a high pressure phase of an ISO event. The pentad mean time series exhibit evident fluctuations on a timescale ranging from 4 to 8 pentads. For each individual event,

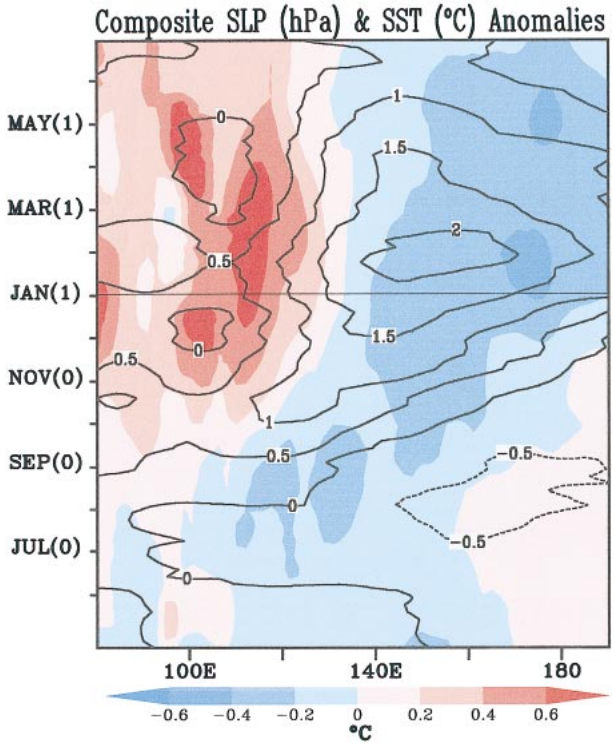

FIG. 2. Longitude–time diagram of the monthly mean sea level pressure (contours) and SST/land surface temperature (color shading) anomalies averaged for the latitude belt between 10° and 20°N. The anomaly fields are composed of the six major El Niño events shown in Fig. 1. The time ordinate runs from May of year 0 to Jul of year 1, where the 0 and 1 denote the year during which ENSO warming develops and decays, respectively. The temperature between 100° and 110°E is primarily the land surface temperature.

the transition of the 7-pentad mean SLP (which represents the slow interannual variation) from below to above normal is rapid due to its association with a swing of an ISO cycle from a low to high pressure phase. As a result, the composite 7-pentad running mean exhibits an increase of SLP by about 5 hPa from −2 to +2 pentad.

The abrupt establishment of the PSAC also shows a close link with the cold air outbreak from the midlatitudes. The vertical bars in Fig. 3 show pentad mean 850-hPa meridional wind anomalies averaged over the southeast coast of China and the neighboring marginal seas (15°–30°N, 110°–130°E). During the low pressure phase before the transition, the prevailing anomalous northerly over that region indicates an intrusion of cold air from continental Asia into the Philippine Sea.

Figure 3 also reveals that the ISO is energetic before and during the anomalous PSAC establishment but inactive after November when the background SLP rises from below to above annual mean (Fig. 1). Computation of the variance of the ISO components averaged over (10°–20°N, 120°–150°E) shows that the composite intensity of ISO is enhanced from May to September before the anomalous PSAC is established, but it is weak-

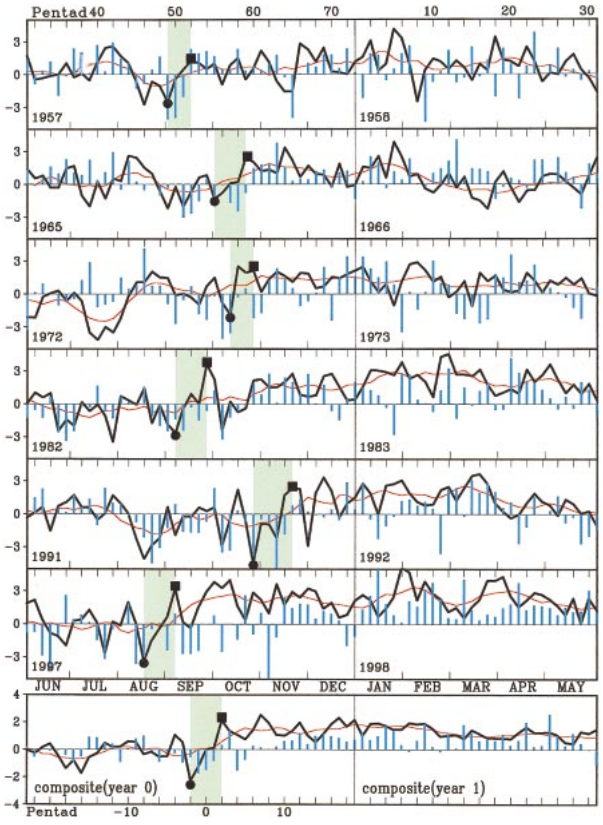

FIG. 3. Pentad mean anomaly (thick black) and the corresponding 7-pentad running mean anomaly (thin red) of the sea level pressure averaged over the Philippine Sea (10°–20°N, 120°–150°E) for six major ENSO warm events and their composite. The composite was made with reference to the transition phase of the establishment period (marked by the green intervals) of the anomalous PSAC. The filled circle and square represent, respectively, the low and high pressure phases of the ISO associated with the formation of the PSAC. The blue vertical bars at each pentad denote the meridional wind anomalies (m s^{-1}) averaged over (15°–30°N, 10°–130°E). The tick marks on the top of each panel denote Julian pentad.

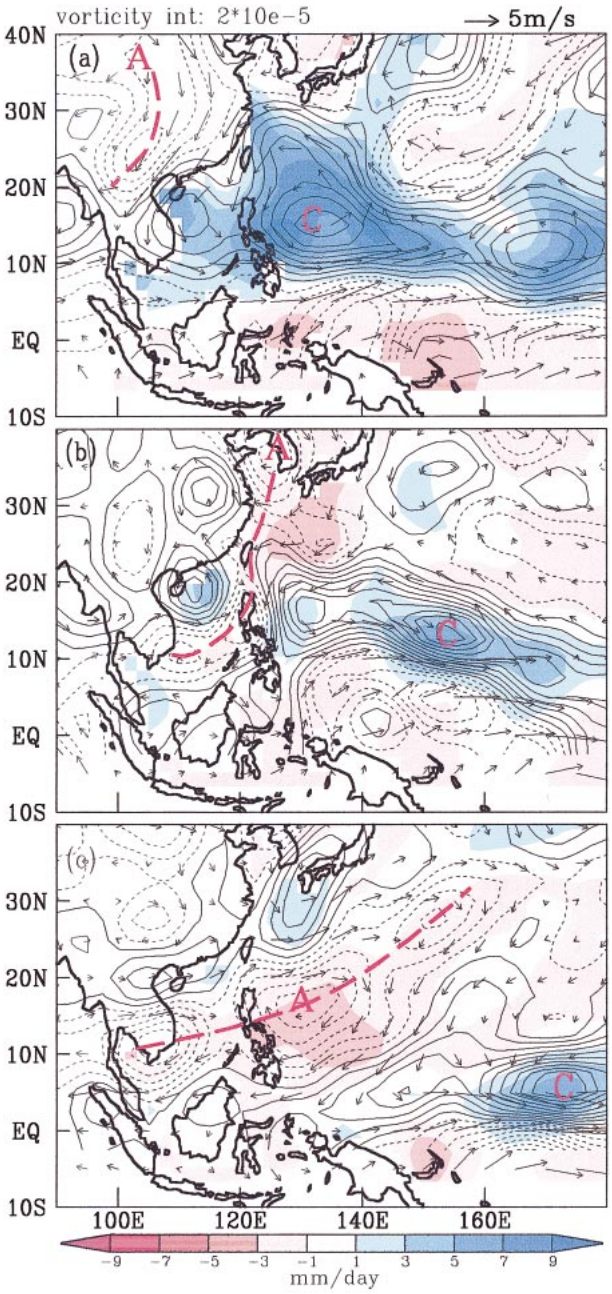

FIG. 4. Composite pentad mean surface wind (arrows) and vorticity (contours in units of 2×10^{-5} s^{-1}) anomalies as well as precipitation rate anomalies (color shading in units of mm day^{-1}) during the (a) low pressure, (b) transition, and (c) high pressure phases of the intraseasonal oscillation associated with the PSAC formation. Letters "A" and "C" mark the centers of the anomalous anticyclone and cyclone, respectively. All fields are composed of the 1982/83, 1991/92, and 1997/98 episodes.

ened after the PSAC establishment from October to the following June (figure not shown). This is particularly evident for the strong events such as the 1965/66, 1972/73, 1982/83, and 1997/98 episodes.

In Fig. 4, we present a composite scenario of the PSAC formation to show features common to all strong El Niño events. At pentad −2 (the low pressure phase of the ISO), a major cyclonic anomaly is centered at (15°N, 130°E). Precipitation is enhanced over the cyclone and the positive vorticity region, indicating a peak convective phase of the ISO. About 2 pentads later, the aforementioned cyclone and associated rainfall anomalies are drastically reduced and the weakened cyclone center moves to (13°N, 150°E). By pentad +2 (the high pressure phase), an anticyclonic anomaly replaces the original cyclonic anomaly and the rainfall is suppressed (dry phase of the ISO), completing a swing from the low to high pressure phase.

In the next three sections, we discuss (i) how the remote forcing produced by the east-central tropical Pacific warming affects the processes of the PSAC establishment, (ii) why the establishment occurs in the fall along with an advanced seasonal transition in east Asia and WNP (or why not in the summer when the remote

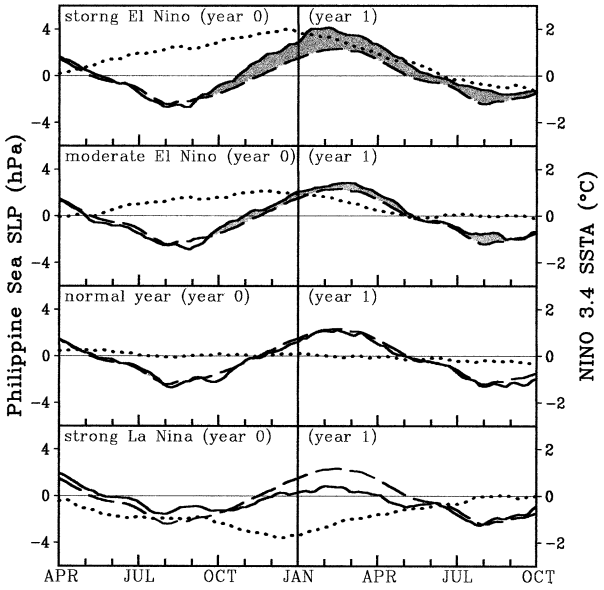

FIG. 5. Same as Fig. 1 except for composite strong El Niño years (1957, 1965, 1972, 1982, 1991, and 1997); moderate El Niño years (1963, 1968, 1976, 1986, 1987, and 1994); normal years (1959, 1960, 1961, 1979, 1990, and 1993); and strong La Niña years (1970, 1973, 1975, 1988, 1998, and 1999).

forcing in the central-eastern Pacific has already reached a considerable amplitude), and (iii) what roles the ISO plays and why, before and during the establishment of PSAC, the ISO has large amplitude, while it tends to damp after November as the PSAC is steadily established. Addressing these questions will provide clues for the physical mechanisms that are important for the PSAC formation.

4. Roles of the remote ENSO forcing in the Tropics

Figure 5 shows how the strength of the anomalous PSAC relates to the intensity of ENSO forcing. For normal years, the Philippine Sea SLP is also normal. The strength of the PSAC increases with increasing amplitude of the El Niño (cf. the composite moderate El Niño with strong El Niño composite in Fig. 5). Conversely, during strong La Niña years, cyclonic anomalies develop over the Philippine Sea. This compelling evidence indicates that the occurrence and intensity of the PSAC depend on the strength of the El Niño forcing.

Figure 6 presents the composite monthly mean 850-hPa wind, precipitation, and SST anomalies before and after the anomalous PSAC establishment. In August, an anomalous cyclone dominates the Philippine Sea. In September, the cyclone weakens while significant anomalous northerlies occur along the east China coast and reach the northern Philippines, indicating a stronger than normal retreat of the east Asian summer monsoon. During October, an anomalous anticyclone emerges over the northern South China Sea and Philippines. By November a well-established anomalous anticyclone controls the tropical and subtropical WNP.

In August (or the summer of the El Niño developing year), the Philippine Sea is dominated by cyclonic, rather than anticyclonic, wind anomalies. This is because the El Niño–induced anomalous westerly in the equatorial west-central Pacific generates strong positive shear vorticity, enhancing precipitation and cyclonic anomalies over the Philippine Sea (Fig. 6a). The cyclonic anomaly enhances the WNP monsoon trough and increases the total wind speed and partially contributes to the local sea surface cooling. This is evidenced by the enhancement of the negative SST anomalies in August and September where the climatological WNP monsoon westerly occurs (Figs. 6a,b). The enhanced precipitation and cloudiness could reduce solar radiation that also adds to the WNP cooling. The lower than normal SST in the vicinity of Philippines preconditions the formation of the anomalous Philippine high in October.

From August to October the reversal of the anomalous vorticity from cyclonic to anticyclonic in the vicinity of Philippines is conceivably caused in part by eastward advection of anomalous anticyclonic vorticity by south Asian monsoon westerlies. In September, an anticyclonic vorticity anomaly occurs over India and the Bay of Bengal (Fig. 6b). This is due to the fact that the anomalous heat sink over the Maritime Continent (the sinking branch of the anomalous Walker circulation) excites descent Rossby waves, which enhance the low-level anticyclonic vorticity on their journey to the west (Gill 1980). The monsoon westerly in south Asia continuously transports the anitcyclonic anomalies toward the South China Sea and the Philippines, favoring the subsequent formation of the anticyclonic anomaly in October.

Accompanying the formation of the Philippine anomalous anticyclone, the rainfall in the vicinity of the Philippines is suppressed and the equatorial easterlies intensify markedly over Borneo, Sumatra, and the equatorial Indian Ocean (Fig. 6c). Meanwhile, the equatorial westerly anomalies and the precipitation anomalies in WNP displace eastward by about 20° longitude (Fig. 6c). This could in part contribute to the slow eastward migration of the anomalous Philippine anticyclone and cold SST anomalies from October to the next February (Fig. 2).

5. Role of the tropical–extratropical interaction

Because the establishment of the PSAC takes place rapidly (usually within 3–5 pentads; Fig. 3), it is conceivable that the atmospheric processes play an essential role in triggering such an abrupt development. As shown in Fig. 4a, at the low pressure phase of the ISO, an anticyclone dominates continental China and *northerly anomalies* along the eastern coast of China penetrate into the South China Sea and the northern Philippines. It is evident that from the low pressure or wet phase

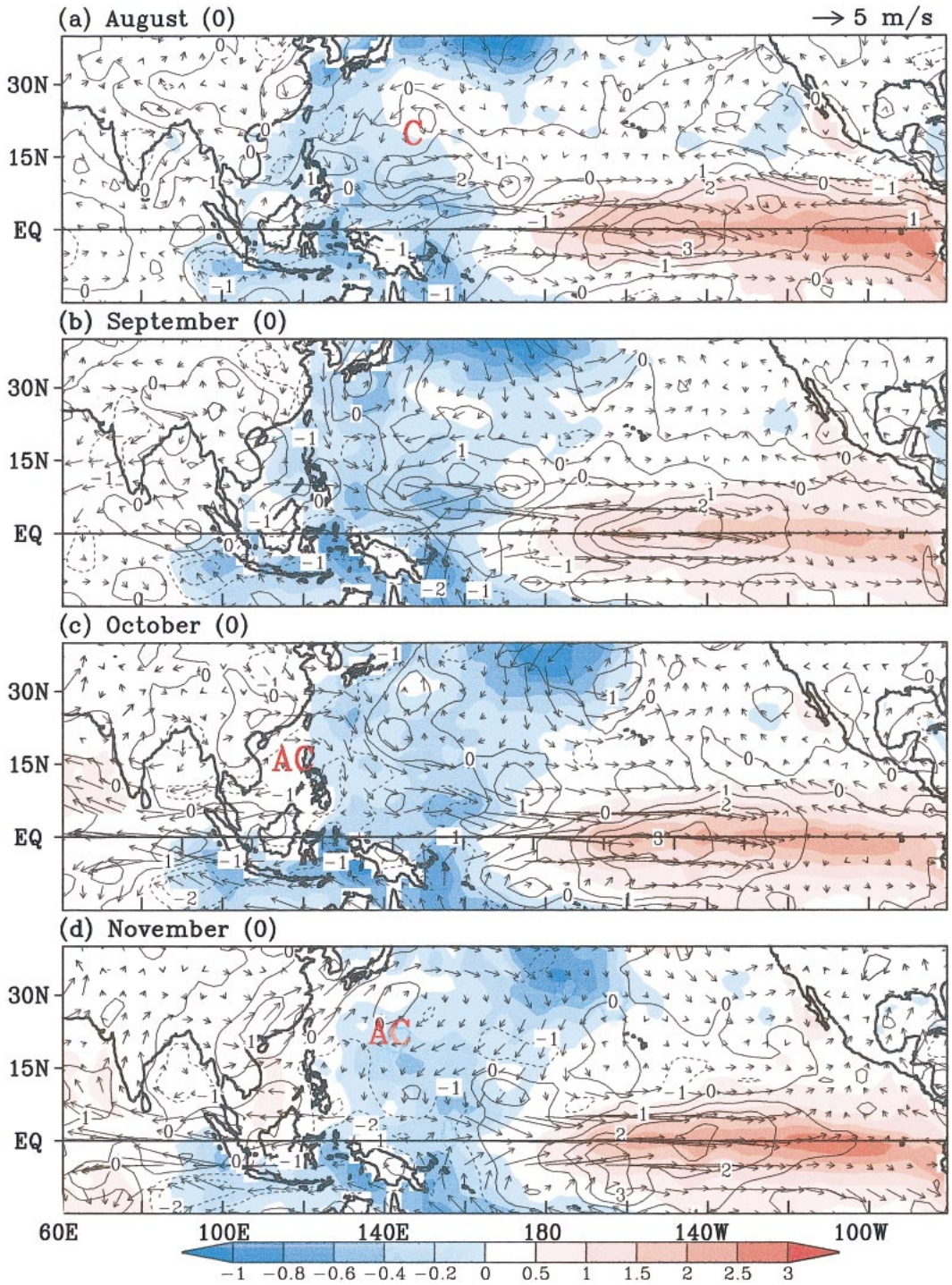

FIG. 6. Composite monthly mean 850-hPa wind (arrows), precipitation rate (contours, mm day^{-1}) and SST (color shading, °C) anomalies for the six strong El Niño events during (a) Aug, (b) Sep, (c) Oct, and (d) Nov of the development year.

(Fig. 4a) to the high pressure or dry phase (Fig. 4c) of the ISO, both the cyclonic and anticyclonic vorticity centers move systematically southeastward, but the cyclonic anomalies abate while the anticyclonic anomaly strengthens. In the transition phase (Fig. 4b), an anomalous anticyclonic ridge extends from the Yellow Sea to the northern Philippines. This anticyclonic ridge originated in central China (Fig. 4a) and subsequently mi-

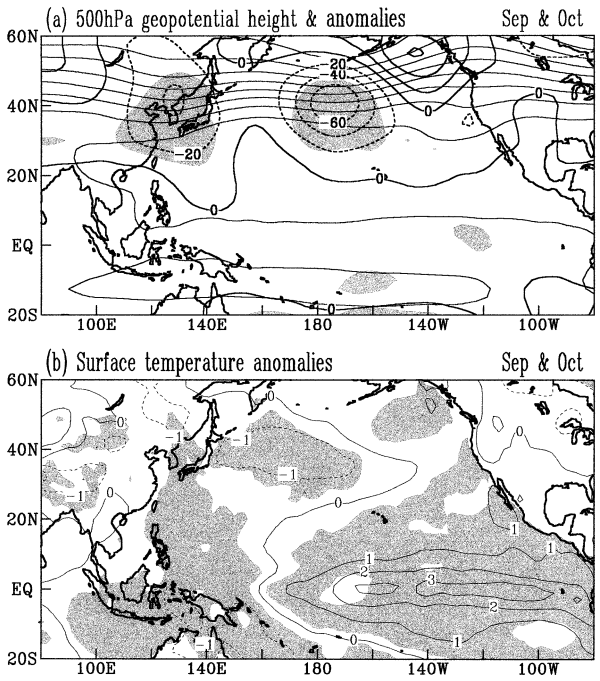

FIG. 7. The differences between the composite strong El Niño and La Niña events (El Niño minus La Niña) in Sep and Oct (a) 500-hPa geopotential height (thin lines) and anomalies (thick lines) and (b) the surface temperature anomalies (°C). Negative values have dashed contours. In (a) superposed on the difference field is the climatological mean 500-hPa geopotential height (thin lines). Contour interval is 20 m. The strong El Niño (La Niña) events used for composite include 1957, 1965, 1972, 1982, 1991, and 1997 (1970, 1973, 1975, 1988, 1998, and 1999). The shaded areas indicate the regions where the difference between the El Niño and La Niña composite is statistically significant at the 5% confidence level by the two-sample *t* test.

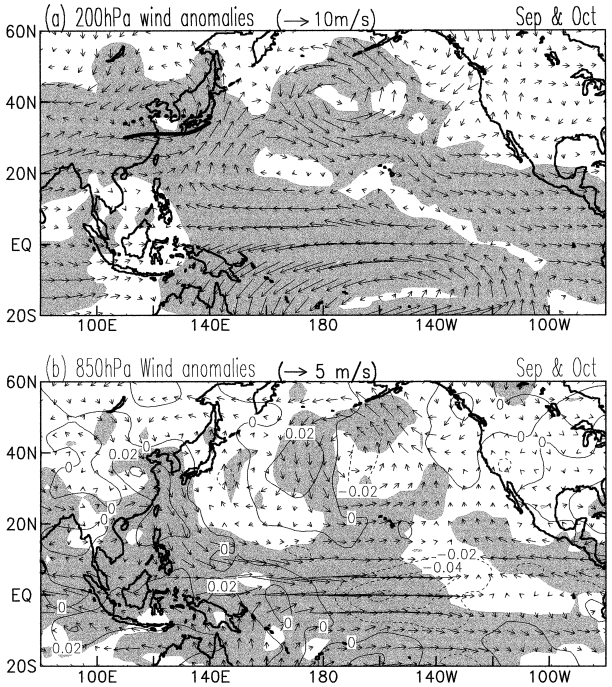

FIG. 8. Same as in Fig. 7 except for (a) 200-hPa wind anomalies and (b) 850-hPa wind anomalies (arrows) and the 500-hPa vertical *p*-velocity anomalies (contours in units of 10^{-3} hPa^{-1}). In (a) the thick solid and dashed line segments show the locations of the Oct mean 200-hPa jet stream axis for the composite strong El Niño and La Niña events, respectively.

grates east over the Philippines (Fig. 4c). We have examined the evolution for each individual event. This transition phase normally accompanies a withdrawal of the east Asian summer monsoon in September–October. The cold air that originated from the midlatitude anticyclone cools the sea surface, providing a triggering mechanism for the abrupt development of PSAC. The northerly anomalies averaged over 15°–30°N, 110°–130°E (the negative vertical bars in Fig. 3) provide evidence to support this proposition.

Why is the cold air activity enhanced in the early fall of the El Niño development year? Figure 7a shows September and October mean 500-hPa geopotential height and the corresponding height difference between the composite strong El Niño and La Niña (El Niño minus La Niña) events. Climatologically, the east Asian trough begins to reestablish in September along the east coast of the Asian continent. The height anomaly shown in Fig. 7a indicates that during a strong El Niño, the east Asian trough tends to be deeper than normal. In accord with this abnormal deepening, the 200-hPa westerly jet extends equatorward. During October of the strong El Niño–developing years, the mean jet axis averaged between 110° and 130°E displaces southward by about 5° latitude compared to that during strong La Niña years (Fig. 8a). The southward displacement of the jet in September and October is favorable for cold air outbreak.

What causes the abnormal deepening of the east Asian trough and southward displacement of the westerly jet during the fall of the strong El Niño years? We propose two possible mechanisms. First, during an El Niño, the Pacific warming-induced anomalous convective heating tends to generate a pair of equatorial symmetric Rossby waves (Gill 1980). At the upper level, an anomalous anticyclonic circulation dominates over the WNP (Fig. 8a). To the northwest of the anticyclonic anomaly anomalous southwesterlies prevail, which perturb the subtropical jet and favor deepening of the east Asian trough between 130° and 150°E. The second reason is related to the anomalous land surface conditions. During the development of El Niño, northeast Asia often experiences a cold summer (Nitta 1987; Tsuyuki and Kurihara 1989; Ferranti et al. 1997; Kang and Jeong 1996; Ropelewski and Halpert 1996; Tanaka 1997). Figure 7b confirms that the land surface cooling weakens but continues in September and October. Note that the abnormal land surface cooling in July and August leads the abnormal deepening of the east Asian trough in September and October. Thus we infer that the cooling of the northeast Asian land facilitates the early formation of the surface high and the deepening of the east Asian trough

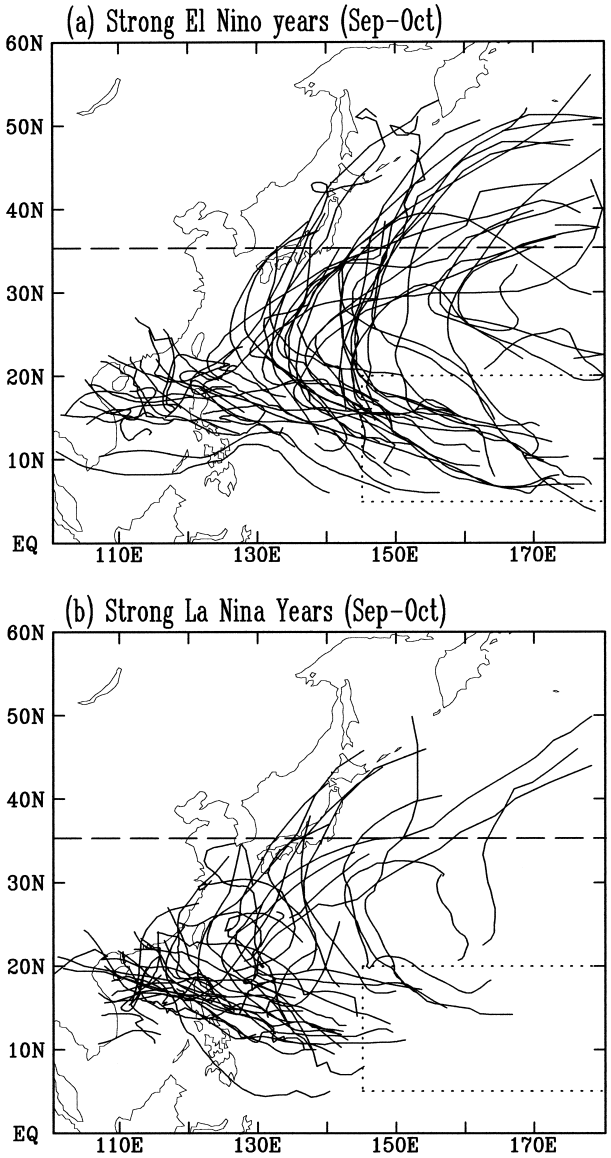

FIG. 9. Tropical storm tracks during the period of 1 Sep to 31 Oct for (a) six major El Niño years (1957, 1965, 1972, 1982, 1991, and 1997) and (b) six major La Niña years (1970, 1973, 1975, 1988, 1998, and 1999). The dotted lines outline the boundaries of the southeast quadrant of the WNP domain. The dashed lines are drawn along 35°N.

by reducing upward transport of sensible heat and the air temperature in the lower troposphere.

The development of El Niño also enhances tropical cyclone activity over the WNP, especially the northward transport of heat by the tropical storms. As is shown in Fig. 8b, during El Niño years, the anomalous low-level equatorial westerly anomalies in the western Pacific generate strong positive shear vorticity, resulting in an eastward extension of the monsoon trough, which in turn causes an eastward displacement of the tropical storm formation as shown by previous studies (e.g., Chen et al. 1998; Chan 2000). Wang and Chan (2002) found that the average life span of the tropical storms during the strong El Niño years is about 7 days, while during the strong La Niña years it is only about 4 days. This is because the storms formed in the southeast quadrant last longer and take a more recurvature path as shown in Fig. 9. Even though the total number of tropical storms formed in the entire WNP (5°–30°N, 120°–180°E) has an *insignificant* difference between the El Niño and La Niña years (Lander 1994), due to the difference in their life spans, the frequency of occurrence of the tropical storms in El Niño years is substantially higher than that in La Niña years. Figure 9 confirms this assertion and shows a sharp contrast in the formation location and the tracks of the tropical storms between the strong El Niño and La Niña years. It is important to notice that in September and October of the six strong El Niño years, the total number of tropical storms that formed in the southeast quadrant of the WNP (5°–20°N, 145°–180°E) is 32, whereas in the six strong La Niña years it is only 9. In addition, during strong El Niño years, more tropical storms recurve northward over the WNP between 125° and 150°E: there are 25 recurved storms reaching 35°N in the six strong El Niño years, whereas there are only 11 in the six strong La Niña years. The more frequent northward recurvature of tropical storms is consistent with the deepening of the 500-hPa east Asian trough. Thus, the El Niño causes energetic tropical storm activity over the WNP.

The sharp increase in the number of the northward-moving tropical storms implies a drastic increase in the northward transport of the warm and moist air (thus heat and energy) from the low to high latitudes during an El Niño fall. Consequently, this would enhance the exchange of air mass and heat between the Tropics and extratropics. This vigorous exchange favors an intense cold air outbreak and the southward extension of the east Asian trough. In fact, low pressure phases of the ISO accompanying the sharp transitions of the PSAC in the six strong El Niño years all involve typhoons or sequential tropical cyclones in the WNP. That explains the striking drop of SLP over the Philippine Sea before the PSAC establishment (Fig. 3). For example, in mid-August of 1997 before the anomalous PSAC establishment, Supertyphoon Winnie took a recurved track over the WNP. Before turning northward, the Philippine Sea pressure was lower than normal by 3 hPa (Fig. 3). The northward recurvature of Supertyphoon Winnie attracted a cold continental high pressure system moving southeastward to the Philippine Sea, bringing cold air from the extratropics and triggering the PSAC development in September. Thus, following the low pressure phase, the Philippine Sea experiences a sharp rise of pressure as shown in Fig. 3. Therefore, the enhanced tropical–extratropical interaction over east Asia and the WNP sector sets up a favorable large-scale environment for the initiation of the PSAC.

6. Roles of the ISO and monsoon–ocean interaction

Figure 3 indicates that the ISO plays a critical role in the sudden establishment of the PSAC. Also evident is that the ISO is active (inactive) before (after) the establishment of the PSAC, in particular, the commencement of the boreal winter regime. In this section, we propose a mechanism to explain this phenomenon.

a. Air–sea interaction sustaining ISO during boreal summer

We argue that the reversal of circulation and precipitation anomalies from a low to a high pressure (or a wet to dry) phase of the ISO (Fig. 4) is partially caused by a negative feedback between the atmosphere and ocean mixed layer temperature. To back up our argument, we computed surface heat fluxes associated with the establishment process for the three major events (1982, 1991, and 1997) for which the SST field (Reynolds and Smith 1994) includes satellite observations and contains signals of intraseasonal variability. Keep in mind that due to the coarse resolution and the weakness of the composite technique, the obtained composite SST tendency and fluxes would substantially underestimate the intraseasonal SST variability. For this reason, the following results concerning the SST variability are considered qualitative and suggestive. At the low pressure phase of the ISO, the cyclonic wind anomaly reinforces the background cyclonic winds in the WNP monsoon trough, thus increasing total wind speed (shading in Fig. 10a) and the upward surface latent heat flux (contours in Fig. 10a); meanwhile, the active convection reduces the downward solar radiation flux (contours in Fig. 10b). Both factors lead to a loss of heat in the ocean mixed layer (Fig. 10c). Assume that the changes in longwave radiation and sensible heat fluxes are small, thus the total heat flux is the sum of the latent and shorwave radiation fluxes. The area of decreasing SST roughly coincides with the area of negative total surface heat flux anomalies exceeding -30 W m^{-2} (shading in Fig. 10c). Because the heat fluxes are computed from the model cloud and winds while the SST tendency is derived from observations, and because the entrainment and horizontal advection processes that might affect SST variation in the ocean mixed layer are neglected, one does not expect a perfect match between the reanalysis total downward heat flux anomalies and the observed SST tendency (which is poor as pointed out earlier). However, the qualitative agreement between these two fields is inspiring. These physically consistent results suggest that the atmospheric ISO has a significant impact on the underlying ocean surface temperature.

On the other hand, the decreased SST would reduce the convective instability and increase the sea level pressure (Zebiak 1986; Lindzen and Nigam 1987; Wang and Li 1993), favoring transformation to a dry phase (Fig. 11a). This ocean feedback process has been confirmed by numerical experiments with an AGCM, which show that a local negative SST anomaly in the western North Pacific can generate a low-level anticyclonic anomaly (Wang et al. 2000).

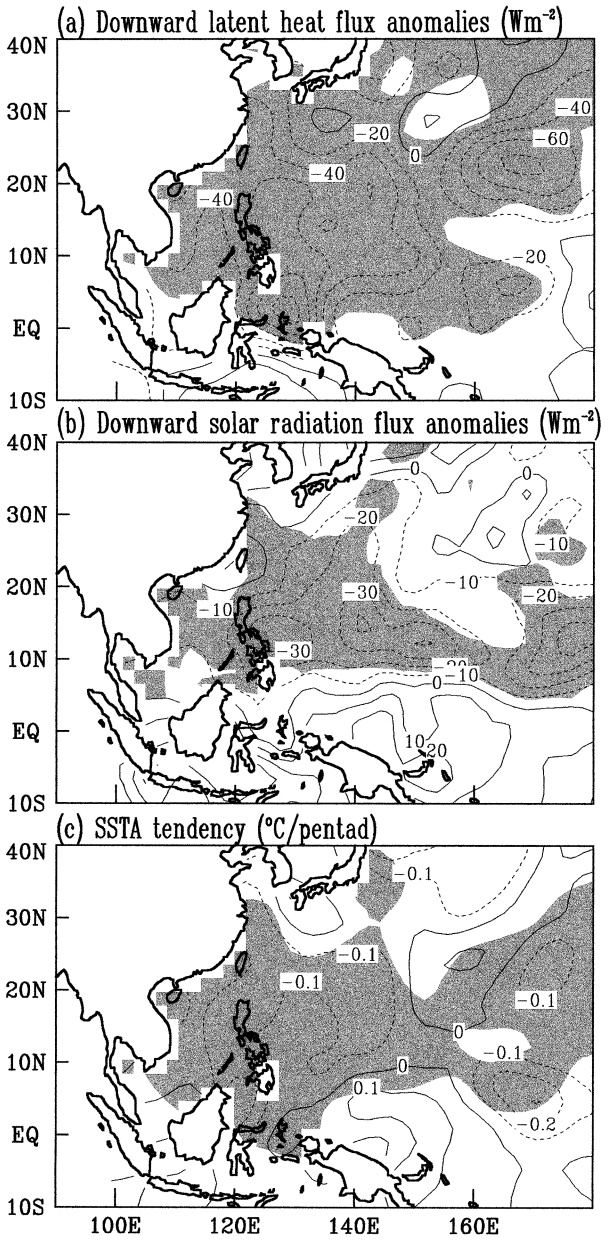

FIG. 10. Composite heat fluxes at the low pressure phase of the ISO associated with the anomalous PSAC formation: (a) downward latent heat flux anomalies (W m^{-2}) with surface wind speed anomalies exceeding 2 m s^{-1} shaded, (b) downward solar radiation flux anomalies (W m^{-2}) with precipitation anomalies exceeding 2 mm day^{-1} shaded, and (c) the SST tendency (°C) with the total downward surface heat flux anomalies exceeding -30 W m^{-2} shaded. All fields are composed of the 1982/83, 1991/92, and 1997/98 episodes.

The aforementioned impact of the low pressure phase of ISO on cooling ocean and the theoretical and nu-

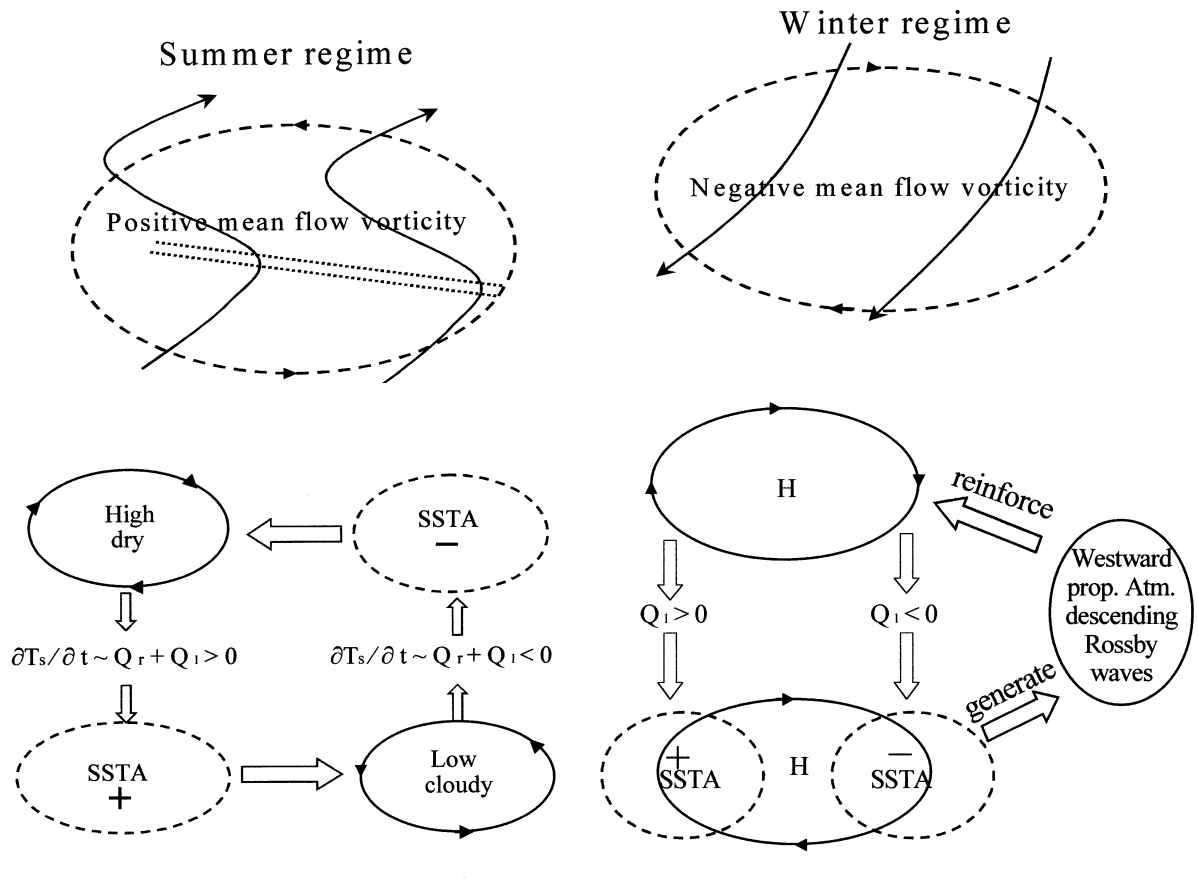

FIG. 11. Schematic diagrams showing the air–sea feedback processes that (a) sustain and (b) damp the ISO depending on the background circulation. Symbols Q_r and Q_l denote, respectively, downward shortwave radiation flux and latent heat flux. The arrow dashed lines and the double dashed lines indicate, respectively, the mean flow and summer monsoon trough.

merical modeling results involving the ocean feedback to ISO lead to the schematic diagram shown in Fig. 11a. When the background flows are controlled by the summer monsoon trough that extends from northern South China Sea toward the central equatorial Pacific (the upper panel of Fig. 11a), a high pressure anomaly would reduce the total wind speed and latent heat loss ($Q_l > 0$) and increase the shortwave radiation heating ($Q_r > 0$) in the mixed layer, thus causing rising SST (Fig. 11a). When the anomalous anticyclone disappears, SST anomalies reach a maximum. The warming then increases convective instability, lowers surface pressure, and activates convection, thus turning the high pressure to a low pressure anomaly. Keeping this circular argument rolling, one finds that as long as the WNP is controlled by the summer monsoon trough, the air–sea interaction through both the cloud–radiation and wind–evaporation/entrainment feedback processes would support the ISO by providing a restoring mechanism.

A theoretical analysis of the effects of these thermodynamic feedbacks on the coupled instability of the warm pool system (in the summer westerly regime) was previously offered by Wang and Xie (1997), who showed that the air–sea thermodynamical coupling may significantly amplify the off-equatorial moist Rossby modes and slow down its propagation. Kemball-Cook and Wang's (2002) numerical experiments with a hybrid coupled ocean–atmosphere model further confirmed this assertion.

b. Why is the ISO inactive after November?

Seasonal march of the SST and mean circulation (e.g., reduction in the vertical easterly shear) are obvious reasons for ISO activity modulation. But how does the change of mean circulations affect the ISO? Does air–sea interaction play a role?

As shown by Wang and Xie (1997), two processes of air–sea interaction over the warm pool ocean may effectively regulate the ISO: one is a feedback through

the cloudiness variation and the other through the surface wind variation. As has been shown in Fig. 10 and Fig. 11a, the cloud–radiation feedback is always a negative feedback thus providing a mechanism to sustain the ISO. This cloud–radiation–SST feedback does not depend on background circulations. On the other hand, the nature of the feedback through surface wind variation unfalteringly depends on background circulation. If the background circulations were cyclonic (summer monsoon regime), as shown by Fig. 10a, the wind–evaporation/entrainment feedback favors maintenance of the ISO. However, if the background circulations were anticyclonic (winter regime), the wind–evaporation/entrainment feedback would tend to demolish the oscillation and maintain the PSAC. The schematic diagram illustrated in Fig. 11b is basically a summary of the theory of Wang et al. (2000), which has been explained in the introduction. What we want to emphasize here is that although the cloud–radiation–SST feedback favors weakening the PSAC, the cooling to the east of the PSAC would continuously suppress convection and generate westward-propagating descending Rossby waves that reinforce the low-level anticyclonic anomalies (the PSAC). Therefore, once the summer monsoon changes to the winter monsoon circulation over the Philippine Sea, the ISO tends to weaken (Fig. 3) and the anomalous PSAC can be maintained until the seasonal circulation changes in the ensuing summer.

The resultant SST pattern has a phase shift with respect to the pressure pattern, that is, the cooling is located to the east of the PSAC and warming to the west (Fig. 11b), which is consistent with observations (Fig. 2). The PSAC and the dipole SST anomaly pattern are, respectively, the atmospheric and oceanic component of the same coupled off-equatorial mode. To test the hypothesis raised by Wang et al. (2000) and illustrated in Fig. 11b, LNW have designed two suites of ensemble experiments with the Geophysical Fluid Dynamics Laboratory (GFDL) AGCM coupled with a mixed layer ocean model. The differences between the two suites of experiments, with and without coupling, convincingly indicated that the local air–sea interaction indeed plays a critical role in maintaining the PSAC and is associated with SST dipole anomalies.

7. Summary

The anomalous Philippine Sea anticyclone (PSAC) is a key system that conveys the impacts of El Niño on the east Asian climate. It not only weakens the east Asian winter monsoon during the mature phase of ENSO, but also brings abundant rainfall in the ensuing spring and summer to the east Asian monsoon front. In this paper, we explore how the PSAC or the El Niño–east Asian teleconnection is established.

a. Conclusions

Analyses of the six major El Niño events reveal the occurrence of the anomalous PSAC leading the maximum Niño-3.4 (5°S–5°N, 120°–170°W) SST anomaly by 2–4 months. On average, it originates in the northern Philippines in late September or October after the east Asian summer monsoon withdraws (Fig. 1). The anticyclone and associated SST cooling to its east migrate together into the Philippine Sea and the western North Pacific (Fig. 2). As a result of the PSAC development, the seasonal transition over the Philippine Sea is advanced. The strength of the PSAC increases with increasing intensity of the Niño-3.4 SST anomalies, whereas, during La Niña, an anomalous *cyclone* develops over the Philippine Sea (Fig. 5).

The establishment of PSAC is rapid, and normally occurs within 3–5 pentads, suggesting that a triggering mechanism is likely rooted in the atmospheric processes. The sudden establishment is found to be associated with a swing of an ISO cycle from a cyclonic to anticyclonic phase (Fig. 3). The ISO, while active before and during the establishment periods, tends to be inactive after the mean circulation changes from summer to winter monsoon.

It was also found that the establishment of the PSAC concurs with (i) intrusion of midlatitude cold air to the Philippines (Fig. 4), (ii) deepening of the upper-level east Asian trough (Fig. 7a), (iii) southward displacement of the upper-troposphere westerly jet (Fig. 8a), and (iv) an increased number of tropical storm formations in the southeast quadrant of the WNP and more frequent northward recurvature of the storm tracks (Fig. 9).

b. Hypothesis and interpretation

The establishment of the anomalous PSAC is attributed to combined effects of remote El Niño forcing, extratropical–tropical interaction, and local air–sea interaction associated with the ISO.

During the summer of the El Niño–developing year, the El Niño–induced central Pacific convection anomalies generate cyclonic circulation anomalies in the Philippine Sea, which increase total wind speed and initiate cold SST anomalies, preconditioning the formation of the Philippine high pressure anomalies (Fig. 6a). On the other hand, the El Niño suppresses Maritime Continent convection through the eastward shift of the Walker circulation. The anomalous heat sink over the Maritime Continent generates anticyclonic vorticity in south Asia (Figs. 6b,c), which is then advected eastward by mean monsoon westerlies, instigating the anomalous anticyclone in the northern Philippines (Fig. 6c).

The strong remote El Niño forcing also influences large-scale east Asian extratropical circulation through a number of processes (see schematic diagram in Fig. 12). Northeast Asia normally experiences a cold El Niño summer (e.g., Nitta 1987; Tsuyuki and Kurihara 1989);

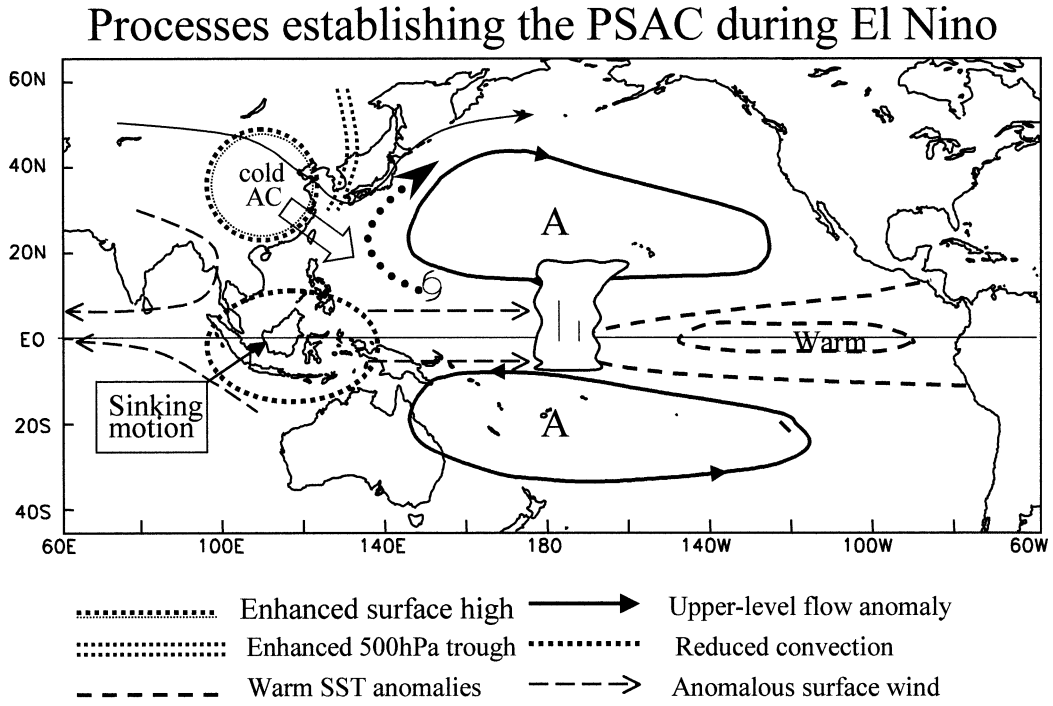

FIG. 12. A schematic diagram illustrating the processes by which remote El Niño–induced tropical–extratropical interaction initiates the anomalous Philippine Sea anticyclone.

the land surface temperature remains below normal in September and October (Fig. 7b). The cold land surface anomaly from summer to early fall would reduce upward sensible heat flux and cool the atmosphere above, resulting in a deeper than normal upper-level trough (Fig. 7a) and a southward shift of the east Asian jet stream in September and October (Fig. 8a). Furthermore, the central Pacific heating anomaly generates westward-propagating ascending Rossby waves, resulting in a low-level cyclonic anomaly and an upper-level anticyclonic anomaly over the WNP (Fig. 8). The upper-level anticyclone perturbs the subtropical westerly jet and enhances southwesterly wind in front of the east Asian trough (Fig. 8a). The low-level cyclonic shear anomalies amplify and extend the WNP monsoon trough farther eastward (Fig. 8b). As a result, tropical storms form more frequently than normal in the southeast quadrant of the WNP (5°–20°N, 145°–180°E) and the number of northward recurving tropical storms increases remarkably (Fig. 9; also Wang and Chan 2002). Thus, the mass and heat exchanges between the Tropics and extratropics are enhanced, which favors cold air bursting from the midlatitude to the Philippine Sea (refer to the negative blue bars in Fig. 3 and anomalous winds in Figs. 4a,b). When the anticyclonic anomaly associated with the enhanced cold air outbreak moves over the Philippine Sea, it cools the SST, triggers the formation of the PSAC, and accelerates the seasonal transition.

During the anomalous PSAC establishment, the ISO plays an essential role in accounting for its abruptness. The in situ air–sea interaction may strongly regulate ISO activity. The cloud–radiation–SST feedback provides a negative feedback to support ISO (Figs. 10b and 11a), while the wind–evaporation/entrainment feedback can either sustain or suppress ISO depending on the background circulation. In the presence of the summer monsoon trough, it helps to maintain ISO (Fig. 10a) but damps ISO after the winter northeasterly trades/winter monsoon commences (Fig. 11b). This explains why the ISO tends to be active before and during the establishment of the PSAC, whereas it is inactive after the late fall. This hypothesis has been supported by the theoretical analysis of the coupled instability of the Rossby wave–ocean interaction (Wang and Xie 1997) and validated by the numerical experiments performed using an coupled AGCM–intermediate ocean model (Kemball-Cook and Wang 2002).

c. Discussion

The results presented here and in Wang et al. (2000) suggest that, in addition to remote ENSO forcing and land surface anomalies, *the monsoon–ocean interaction may play an important role in Asian summer monsoon variations.* This assertion has been corroborated by the numerical experimental results with a coupled general circulation model at GFDL (Lau and Nath 2000). In their recent numerical experiments using the GFDL coupled AGCM and the mixed layer ocean model, LNW demonstrated that the local air–sea interaction in the

WNP warm pool could indeed generate and maintain the PSAC.

The air–sea interaction involved in the boreal summer ISO over the WNP was documented using the NCEP–NCAR reanalysis dataset (Kemball-Cook and Wang 2001). The results are believed to be qualitatively valid; we are currently extending this study using high-resolution satellite observations. However, many of the arguments about the nature of the air–sea interaction on intraseasonal timescales over the off-equatorial warm pool regions deserve further investigation using more supplicated coupled models.

We show for the first time firm evidence that the establishment of the PSAC is about one season earlier than the peak warming in the eastern-central equatorial Pacific. This phase lead has important implications for the possible role of the PSAC in the El Niño turnabout (Wang et al. 1999). After the establishment of the PSAC, the easterly anomalies associated with the PSAC dominate the Maritime Continent and the far western equatorial Pacific (Fig. 6d). Using the NCEP–NCAR ocean reanalysis data, Wang et al. (2001) have shown that such a sudden change of equatorial zonal winds induces a sequence of oceanic upwelling Kelvin waves that propagate eastward and erode the warming on their journey to the eastern Pacific. Accumulative effects of these upwelling Kelvin waves may play an active role in accelerating the turnabout of the ENSO cycle (Kessler and McPhaden 1995; Weisberg and Wang 1997). This, in part, explains why all major ENSO warmings are characterized by a rapid decay after their mature phase when the PSAC is firmly established and why the ENSO turnabout prefers to occur in the northern winter (Wang et al. 2001; An and Wang 2001).

The formation of the Philippine anticyclone in the fall of El Niño development is an important yet intriguing issue. Other ideas should not be neglected. Nigam (1994) has shown that El Niño–induced mean flow variation could interact with topography and affect the Indian summer monsoon. Watanabe and Jin (2002), are exploring the impact of the Tibetan Plateau on the ENSO-induced tropical circulation change, which could influence downstream circulation anomalies. In this study, we focus on common features of El Niño–east Asian teleconnection, but the evolution of El Niño events appears to exhibit interdecadal modulations. This is reflected in the intensity of the PSAC between the strong events before and after the late 1970s (Figs. 1 and 3). The change of the ENSO–east Asian monsoon relationship deserves further study. Recent works of Chang et al. (2000) and Wu and Wang (2002) have accumulated useful knowledge in this regard.

Acknowledgments. We thank Dr. N.-C. Lau for stimulating discussions. This work has been supported by NOAA OGP/Pacific Program and the Climate Dynamics Program, National Science Foundation Award ATM-00-73023. The International Pacific Research Center is sponsored in part by the Frontier Research System for Global Change.

REFERENCES

An, S.-I., and B. Wang, 2001: Mechanisms of locking the El Niño and La Niña mature phases to boreal winter. *J. Climate,* **14,** 2164–2176.

Chan, J. C. L., 2000: Tropical cyclone activity over the western North Pacific associated with El Niño and La Niña events. *J. Climate,* **13,** 2960–2972.

Chang, C.-P., Y. S. Zhang, and T. Li, 2000: Interannual and interdecadal variations of the East Asian summer monsoon and tropical Pacific SSTs. Part I: Role of subtropic ridges. *J. Climate,* **13,** 4310–4325.

Chen, T.-C., S.-P. Weng, N. Yamazaki, and S. Kiehne, 1998: Interannual variation in the tropical cyclone formation over the western North Pacific. *Mon. Wea. Rev.,* **126,** 1080–1090.

Ferranti, L., J. M. Slingo, T. N. Palmer, and B. J. Hoskins, 1997: Relations between interannual and intraseasonal monsoon variability as diagnosed from AMIP integrations. *Quart. J. Roy. Meteor. Soc.,* **123,** 1323–1357.

Gill, A. E., 1980: Some simple solutions for heat-induced tropical circulation. *Quart. J. Roy. Meteor. Soc.,* **106,** 447–462.

Gu, D., and S. G. H. Philander, 1997: Interdecadal climate fluctuations that depend on exchanges between the Tropics and the extratropics. *Science,* **275,** 805–807.

Huang, R.-H., and Y.-F. Wu, 1989: The influence of ENSO on the summer climate change in China and its mechanism. *Adv. Atmos. Sci.,* **6,** 21–32.

Kalnay, E., and Coauthors, 1996: The NCEP/NCAR 40-Year Reanalysis Project. *Bull. Amer. Meteor. Soc.,* **77,** 437–471.

Kang, I., and Y. Jeong, 1996: Association of interannual variations of temperature and precipitation in Seoul with principal modes of Pacific SST. *J. Korean Meteor. Soc.,* **32,** 339–345.

Kawamura, R., 1998: A possible mechanism of the Asian summer monsoon–ENSO coupling. *J. Meteor. Soc. Japan,* **76,** 1009–1027.

Kemball-Cook, S., and B. Wang, 2001: Equatorial waves and air–sea interaction in the boreal summer intraseasonal oscillation. *J. Climate,* **14,** 2923–2942.

——, and ——, 2002: Simulation of the intraseasonal oscillation in the ECHAM-4 model: The impact of coupling with an ocean model. *J. Atmos. Sci.,* **59,** 1433–1453.

Kessler, W. S., and M. J. McPhaden, 1995: Oceanic equatorial waves and the 1991–1993 El Niño. *J. Climate,* **8,** 1757–1774.

Lander, M. A., 1994: An exploratory analysis of the relationship between tropical storm formation in the western North Pacific and ENSO. *Mon. Wea. Rev.,* **122,** 636–651.

Lau, K.-M., and S. Yang, 1996: The Asian monsoon and predictability of the tropical ocean–atmosphere system. *Quart. J. Roy. Meteor. Soc.,* **122,** 945–957.

Lau, N.-C., and M. J. Nath, 2000: Impact of ENSO on the variability of the Asian–Australian monsoons as simulated in GCM experiments. *J. Climate,* **13,** 4287–4309.

Lindzen, R. S., and S. Nigam, 1987: On the role of sea surface temperature gradients in forcing low-level winds and convergence in the tropics. *J. Atmos. Sci.,* **44,** 2418–2436.

Murakami, T., and J. Matsumoto, 1994: Summer monsoon over the Asian continent and western North Pacific. *J. Meteor. Soc. Japan,* **72,** 719–745.

Nigam, S., 1994: On the dynamical basis for the Asian summer monsoon rainfall–El Niño relationship. *J. Climate,* **7,** 1750–1771.

Nitta, T., 1987: Convective activities in the tropical western Pacific and their impacts on the Northern Hemisphere summer circulation. *J. Meteor. Soc. Japan,* **65,** 373–390.

Reynolds, R. W., and T. M. Smith, 1994: Improved global sea surface temperature analyses using optimum interpolation. *J. Climate,* **7,** 929–948.

Ropelewski, C. F., and M. S. Halpert, 1996: Quantifying Southern Oscillation–precipitation relationships. *J. Climate,* **9,** 1043–1059.

Tanaka, M., 1997: Interannual and interdecadal variations of the western North Pacific monsoon and the East Asian Baiu rainfall and their relationship to ENSO cycles. *J. Meteor. Soc. Japan,* **75,** 1109–1123.

Tao, S., and Q. Zhang, 1998: Response of the East Asian summer monsoon to ENSO events (in Chinese). *Sci. Atmos. Sin.,* **22,** 399–407.

Tsuyuki, T., and K. Kurihara, 1989: Impacts of convective activity in the western tropical Pacific on the East Asian summer circulation. *J. Meteor. Soc. Japan,* **67,** 231–247.

Wang, B., 1994: Climatic regimes of tropical convection and rainfall. *J. Climate,* **7,** 1109–1118.

——, 1995: Interdecadal changes in El Niño onset in the last four decades. *J. Climate,* **8,** 267–258.

——, and T. Li, 1993: A simple tropical atmospheric model of relevance to short term climate variation. *J. Atmos. Sci.,* **50,** 260–284.

——, and X. Xie, 1997: A model for the boreal summer intraseasonal oscillation. *J. Atmos. Sci.,* **54,** 72–86.

——, and J. C.-L. Chan, 2002: How strong ENSO events affect tropical storm activity over the western North Pacific. *J. Climate,* **15,** 1643–1658.

——, R. Wu, and R. Lukas, 1999: Roles of the western North Pacific winds in thermocline adjustment and ENSO phase transition. *J. Meteor. Soc. Japan,* **77,** 1–16.

——, ——, and X. Fu, 2000: Pacific–East Asian teleconnection: How does ENSO affect East Asian climate? *J. Climate,* **13,** 1517–1536.

——, ——, R. Lukas, and S. I. An, 2001: A possible mechanism for ENSO turnabout. *Dynamics of Atmospheric General Circulation and Climate,* IAP/Academia Sinica, China Meteorological Press, in press.

Watanabe, M., and F. Jin, 2002: Role of Indian Ocean warming in the development of Philippine Sea anticyclone during ENSO. *Geophys. Res. Lett.,* in press.

Weisberg, R. H., and C. Wang, 1997: Slow variability in the equatorial west-central Pacific in relation to ENSO. *J. Climate,* **10,** 1998–2017.

Wu, R., and B. Wang, 2000: Interannual variability of summer monsoon onset over the western North Pacific and the underlying processes. *J. Climate,* **13,** 2483–2501.

——, and ——, 2002: A contrast of the East Asian summer monsoon–ENSO relationship between 1962–77 and 1978–93. *J. Climate,* **15,** 3266–3279.

Zebiak, S., 1986: Atmospheric convergence feedback in a simple model for El Niño. *Mon. Wea. Rev.,* **114,** 1263–1271.

Zhang, R., A. Sumi, and M. Kimoto, 1996: Impact of El Niño on the East Asian monsoon: A diagnostic study of the '86/87 and '91/92 events. *J. Meteor. Soc. Japan,* **74,** 49–62.